

# Aberration retrieval using the extended Nijboer-Zernike approach

Peter Dirksen<sup>a</sup>, Joseph Braat<sup>b</sup> Augustus J.E.M. Janssen<sup>c</sup>, Casper Juffermans<sup>a</sup>

<sup>a</sup>Philips Research Leuven, Belgium

<sup>b</sup>Delft University of Technology, The Netherlands

<sup>c</sup>Philips Research Laboratories, The Netherlands

## ABSTRACT

In this paper we give the proof of principle of a new experimental method to determine the aberrations of an optical system in the field. The measurement is based on the observation of the intensity point-spread function of the lens. To analyse and interpret the measurement, use is made of an analytical method, the so-called extended Nijboer-Zernike approach. The new method is applicable to lithographic projection lenses, but also to EUV mirror systems or microscopes such as the objective lens of an optical mask inspection tool. Phase retrieval is demonstrated both analytically and experimentally. The extension of the method to the case of a medium-to-large hole sized test object is presented. Theory and experimental results are given. In addition we present the extension to the case of aberrations comprising both phase and amplitude errors.

**Keywords:** Optical lithography, aberrations, phase retrieval, amplitude retrieval, point-spread function, Nijboer-Zernike theory

## 1. INTRODUCTION

The increased interest in qualification methods for lithographic projection lenses may be explained from a number of factors: projection lens aberrations are known to have an important contribution to linewidth variation and image misplacement.<sup>1,2</sup> Their impact gets more pronounced with each new technology node due to the small dimensions compared to the exposure wavelength, i.e. low  $k_1$ -imaging requires tighter aberration specifications. To minimise the impact of aberrations, modern lithographic lenses have a number of manipulators to tune specific aberration terms. Focal plane deviation, astigmatism, coma and spherical aberration are all adjustable quantities. Although the lens manufacturer delivers a well optimised lens, the advanced user needs to balance lens aberrations for optimal performance on specific patterns. In addition, aberrations may vary in time due to lens aging and machine drift.

Although several user tests are available such as an in-situ interferometer<sup>3</sup> or various resist based methods,<sup>4-6</sup> we have chosen for a different approach. Our approach to determine the lens aberrations, both phase and amplitude, is based on the observation of the intensity point-spread function of the lens, a method that has a number of advantages. The test pattern is the most simple and elementary pattern that exists: an isolated transparent hole in a dark field binary mask. For a sufficiently small hole diameter, small compared to the system resolution, the image will approximate the point-spread function of the lens, that is either recorded in resist or captured by a detector. Exposing the mask through focus, results in the measurement of the 3D-intensity of the point-spread function. It is noted that the point-spread function fully characterises the lens and is independent of the illumination source. Also, the point-spread function contains the information of both

---

Further author information:

P.D. and C.J.: E-mail: peter.dirksen@imec.be, Philips Research Leuven, Kapeldreef 75, B-3001 Leuven, Belgium

J.B.: Optics Research Group, Department of Applied Sciences, Delft University of Technology, Lorentzweg 1, NL-2628 CJ Delft, The Netherlands

A.J.E.M.J.: Philips Research Laboratories, WY-81, NL-5656 AA Eindhoven, The Netherlands

This paper is a revised version of "Characterization of a projection lens using the extended Nijboer-Zernike approach", presented at the *SPIE* conference, Vol. 4691 (2002) p 1391

the low and high order aberrations. From an experimental point of view the procedure is straightforward. The problematic part is therefore not the experiment, it is the interpretation of the measurement.

To analyse and interpret the measurement, use is made of a new analytical method. The through-focus image intensity of the point-spread function, including the effects of aberrations, is described by a recently found Bessel series representation. This description, called the extended Nijboer-Zernike approach,<sup>7,8</sup> is tailor made for the inverse problem we have to solve: retrieving the phase defects (aberrations) of the lens from the intensity measurements in the focal region. Following the new approach, the through-focus point-spread function is expressed as a combination of basic functions. The coefficients of these basic functions are identical to the Zernike coefficients that represent the pupil function and are estimated by optimising the match between the theoretical intensity and the measured intensity patterns at several values of the defocus parameter.

Phase retrieval by the extended Nijboer-Zernike approach is applicable to lithographic projection lenses, but also to EUV mirror systems or microscopes such as the objective lens of an optical mask inspection tool. This paper gives a detailed description of the phase retrieval method and shows the first experimental results, demonstrating the feasibility of our approach. The last section discusses the extension to general aberration retrieval. Here we consider the retrieval of general aberrations  $A \cdot \exp(i\Phi)$  with a possible non-constant pupil transmission amplitude  $A$ . Retrieval of amplitude errors is a unique feature of our method and will be worked out in more detail in Ref. [10].

## 2. BASIC FORMULAS FOR THE COMPUTATION OF THE COMPLEX AMPLITUDE OF A POINT-SPREAD FUNCTION

The point-spread function is the image of a mathematical delta function, but in practice an object having a diameter of the order of  $\sim \frac{\lambda}{2NA}$  is a fair approximation. The complex amplitude of a point-spread function is denoted as  $U(x, y)$ . The relationship between normalised image coordinates  $(x, y)$  and the defocus parameter  $f$  and the real space image coordinates  $(X, Y, Z)$  in the lateral and axial direction is given by:

$$\begin{aligned} x &= X \frac{NA}{\lambda} \quad , \quad y = Y \frac{NA}{\lambda} & (1) \\ r &= \sqrt{x^2 + y^2} \quad , \quad (x, y) = (r \cos \phi, r \sin \phi) \\ f &= 2 \frac{\pi}{\lambda} Z (1 - \sqrt{1 - NA^2}) \quad . \end{aligned}$$

Without loss of generality, the usual symmetry and normalization assumptions may be made and we expand the aberration phase  $\Phi$  as a series of Zernike polynomials:

$$\Phi = \sum_{nm} \alpha_{nm} R_n^m(\rho) \cos(m\theta) \quad , \quad \text{with real } \alpha_{nm}, \quad 0 \leq \theta \leq 2\pi, \quad 0 \leq \rho \leq 1. \quad (2)$$

We use the Fringe Zernike convention to represent the lens aberrations, as shown in the table below.

Fringe Zernike convention			
$(n, m)$	Name	$R_n^m(\rho) \cos(m\theta)$	Term
(0,0)	Piston	1	$Z_1$
(1,1)	Tilt	$\rho \cos(\theta)$	$Z_2$
(2,0)	Defocus	$2\rho^2 - 1$	$Z_4$
(2,2)	Astigmatism	$\rho^2 \cos(2\theta)$	$Z_5$
(4,0)	Spherical	$6\rho^4 - 6\rho^2 + 1$	$Z_9$
(3,1)	X-Coma	$(3\rho^3 - 2\rho) \cos(\theta)$	$Z_7$
(3,3)	X-Three point	$\rho^3 \cos(3\theta)$	$Z_{10}$

⋮

For a number of special cases the point-spread function is well known. The in-focus ( $f = 0$ ), aberration-free ( $\alpha_{nm} = 0$ ) amplitude distribution of the point-spread function is the Airy pattern:

$$U(x, y) = 2 \frac{J_1(v)}{v}, \quad v = 2\pi r. \quad (3)$$

A central spot is surrounded by a dark ring corresponding to the first minimum of  $J_1(v)$ . The in-focus ( $f = 0$ ) amplitude distribution in the presence of small aberrations was already given by Nijboer<sup>9</sup> as:

$$\begin{aligned} \text{Spherical } U(x, y) &\approx 2 \left( \frac{J_1(v)}{v} + i \alpha_{4,0} \frac{J_5(v)}{v} \right) \\ \text{Coma } U(x, y) &\approx 2 \left( \frac{J_1(v)}{v} - \alpha_{3,1} \frac{J_4(v)}{v} \cos \phi \right) \\ \text{Astigmatism } U(x, y) &\approx 2 \left( \frac{J_1(v)}{v} - i \alpha_{2,2} \frac{J_3(v)}{v} \cos 2\phi \right) \end{aligned} \quad (4)$$

with  $v = 2\pi r$ . According to the extended Nijboer-Zernike theory,<sup>7, 8</sup> the complex amplitude of the point-spread function  $U$  is in first order approximation given by:

$$U \approx 2V_{00} + 2i \sum_{n,m} \alpha_{nm} i^m V_{nm} \cos m\phi, \quad (5)$$

where  $\alpha_{nm}$  are the Zernike coefficients of the single aberrations  $R_n^m(\rho) \cos m\theta$ . For integers  $n, m \geq 0$  with  $n - m \geq 0$  and even, the Bessel series representation for  $V_{nm}$  reads

$$V_{nm}(r, f) = \exp(if) \sum_{l=1}^{\infty} (-2if)^{l-1} \sum_{j=0}^p v_{lj} \frac{J_{m+l+2j}(v)}{lv^l}, \quad v = 2\pi r, \quad (6)$$

with  $v_{lj}$  given by

$$v_{lj} = (-1)^p (m+l+2j) \binom{m+j+l-1}{l-1} \binom{j+l-1}{l-1} \binom{l-1}{p-j} / \binom{q+l+j}{l}, \quad (7)$$

where  $l = 1, 2, \dots; j = 0, \dots, p$ . In Eq. (7) we have set

$$p = \frac{n-m}{2}, \quad q = \frac{n+m}{2}. \quad (8)$$

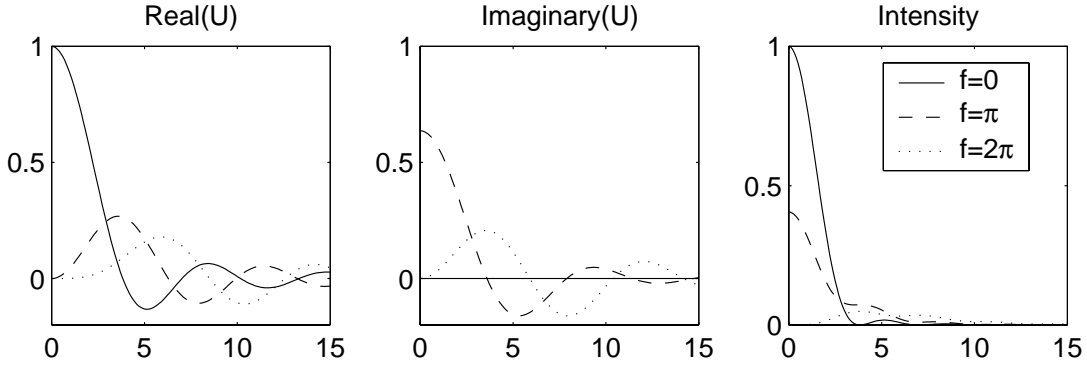
The special case of  $f = 0$  corresponds to Eq. (4). For the number  $L$  of terms to be included in the infinite series over  $l$  the following rule<sup>8</sup> is used: if  $L$  is three times the defocus parameter, the absolute truncation error is of the order  $10^{-6}$ .

Fig. 1 gives a result of the through-focus aberration-free amplitude and intensity distribution of the point-spread function, calculated with Eq. (5).

High-order aberrations, i.e. large values of  $n$  and  $m$  and large defocus values up to  $f = \pm 4\pi$  provide no problem for the convergence of the series in Eq. (6). The extended Nijboer-Zernike approach is therefore tailor-made for our phase retrieval problem and for the description of short-range stray light in the image plane.

## 2.1. Extension to finite hole size

Up to now we have assumed that the diameter of the hole in the binary mask is so small that it can be regarded as a true delta function. From a practical point of view, however, it would be favourable to use holes with a non-negligible diameter since the increased amount of light would significantly reduce the required exposure dose, making the experimental procedure much more practical. We assume that the diameter is small compared to the coherence radius of the illumination source, a condition that is almost always fulfilled. The effect of a



**Figure 1.** The through-focus aberration-free amplitude and intensity distribution of the point-spread function. The horizontal axis represent the radial axis in normalised units, see Eq. (1)

non-negligible diameter is a drop in amplitude at the rim of the pupil. In normalized coordinates, this means that the pupil function must be multiplied by the Fourier transform of a disk

$$\frac{J_1(2\pi a\rho)}{\pi a\rho}, \quad 0 \leq \rho \leq 1, \quad (9)$$

with  $a$  the normalized diameter of the hole. Here one should think of  $a$  as large as  $1/\pi$  so that an amplitude drop of some 40 % at the rim  $\rho = 1$  of the pupil results from multiplication by the function in Eq. (9). In fact, in the experiments described in Sec. 3.2 we have used holes with a diameter of  $0.6\mu\text{m}$  which corresponds to a normalized diameter  $a$  of  $\frac{NA}{2\pi\lambda} * \text{diam} \sim 0.31$ .

The extended Nijboer-Zernike theory is sufficiently flexible to account for this effect.<sup>10</sup> Here one approximates

$$\frac{J_1(2\pi a\rho)}{\pi a\rho} \approx \exp(c - d\rho^2), \quad (10)$$

with optimal  $c, d$ , and the  $V_{nm}(r, f)$  of Eq. (6) should be replaced throughout by

$$\exp(c)V_{nm}(r, f + id) \quad (11)$$

As one sees from Eq. (6), nothing prevents us from using the Bessel series representation with complex defocus parameter  $f + id$ . The optimal  $c, d$  in Eq. (10) are accurately given as a function of  $b = 2\pi a$  by

$$c = \frac{b^4}{2304} + \frac{b^6}{46080}, \quad d = \frac{b^2}{8} + \frac{b^4}{384} + \frac{b^6}{10240} \quad (12)$$

A similar correction can be carried out in the case the conventional approximation  $\exp(if\rho^2)$  is no longer adequate due to high numerical aperture, see Ref. [10] for further details. Accordingly, the application range of the method is extended from NA of around 0.65 to NA up to 0.85. Figure 2 shows a comparison of the extended Nijboer-Zernike theory and a commercial lithographic simulator (Solid-c). As an example we chose an aberration-free lens, two settings of the numerical aperture  $NA = 0.6$  and  $NA = 0.80$  and two diameters of  $0.1\mu\text{m}$  and  $0.3\mu\text{m}$ . The intensity deviations between the analytical computation and the Solid-c full vectorial, unpolarized calculation has a standard deviation typical of the order of  $\sim 1\%$ . A detailed assessment and additional examples can be found elsewhere.<sup>8,10</sup>

## 2.2. Determination of the Zernike coefficient: phase retrieval

At first sight it seems impossible to retrieve the aberrations from an intensity measurement as all phase information is lost in passing from complex amplitude to intensity. Below we will show that this is not the case.

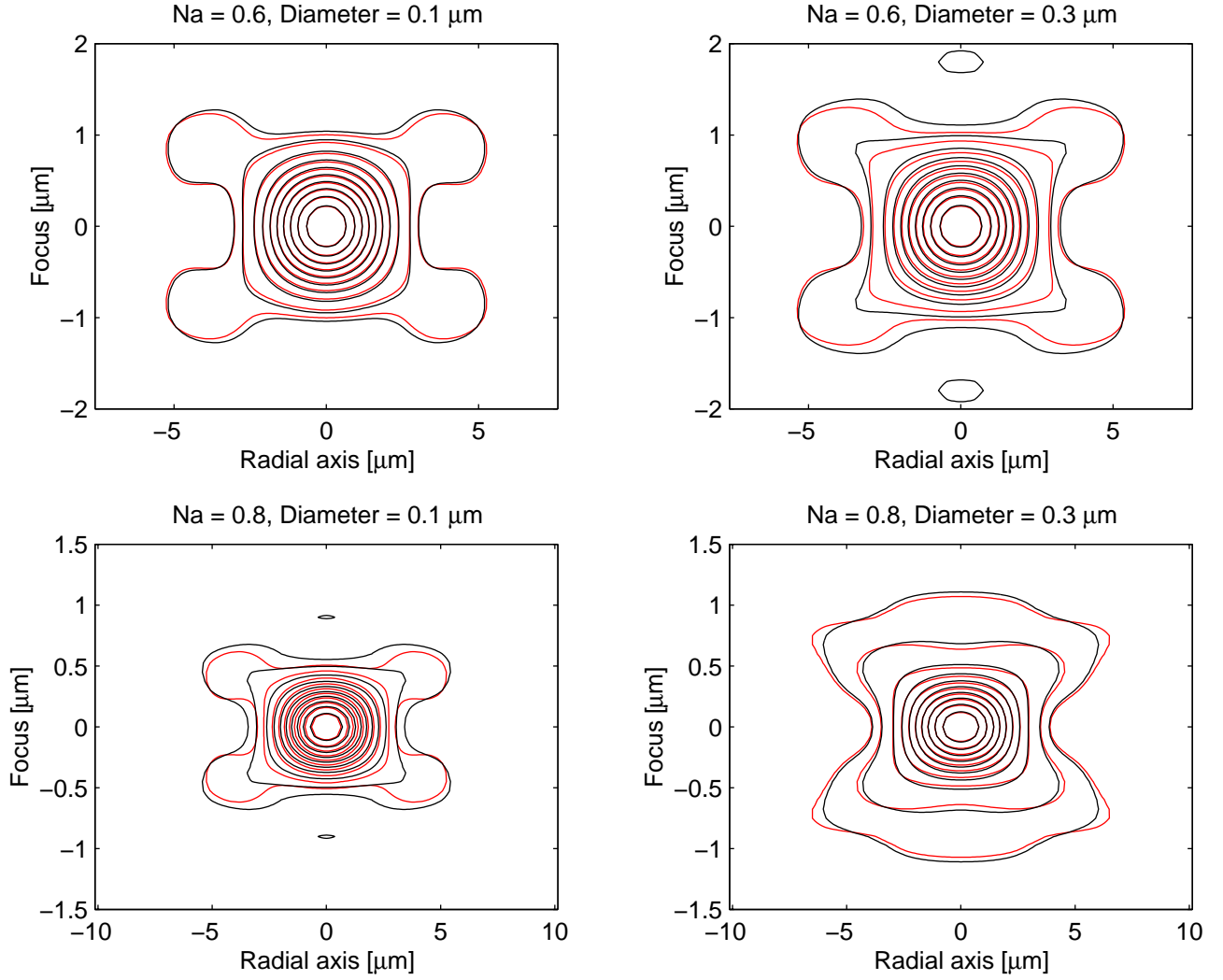


**Figure 2.** The point-spread function of an aberration-free lens for various values of the numerical aperture and hole size. The extended Nijboer-Zernike theory is compared with a commercial lithographic simulator (Solid-c). The deviations are typically 1 %.

The observed quantity is the *image intensity*  $I(x, y, f) = |U(x, y, f)|^2$ . Usually the image intensity is measured using rectangular coordinates. The first step is to transform the observed image intensity to polar coordinates  $I(r, \phi, f)$ . Using Eq. (5), the intensity is in a first order approximation:

$$I \approx 4|V_{00}|^2 + 8 \sum_{nm} \alpha_{nm} \text{Re}\{i^{m+1} V_{00}^* V_{nm}\} \cos m\phi \quad (13)$$

It is our task to estimate the Zernike coefficients  $\alpha_{nm}$  from  $I$ .

A Fourier analysis with respect to the angular dependence of the observed image intensity is made:

$$\Psi^m(r, f) = \frac{1}{2\pi} \int_0^{2\pi} I(r, \phi, f) \cos m\phi d\phi \quad (14)$$

An inner product is defined in the  $(r, f)$  space:

$$(\Psi, \chi) = \int_0^R \int_{-F}^F r \cdot \Psi(r, f) \cdot \chi(r, f)^* drdf \quad (15)$$

We denote:

$$\Psi_n^m(r, f) = \gamma_m \text{Re}\{i^{m+1} V_{00}^* V_{nm}\}, \quad (16)$$

with  $\gamma_m = 4$ ,  $m = 1, 2, \dots$ ,  $\gamma_0 = 8$ . Then by multiplying Eq. (13) by  $\cos m\phi$  and integrating over  $\phi$ , the  $m^{\text{th}}$ -harmonic of the observed intensity is expressed as a linear sum of the  $\Psi_n^m(r, f)$  functions with coefficients  $\alpha_{nm}$ :

$$\sum_n \alpha_{nm} \Psi_n^m(r, f) = \Psi^m(r, f) \quad (17)$$

By taking the inner product, defined above, of Eq. (17) with  $\Psi_{n'}^m$ , the Zernike coefficients can be found on solving a linear system of equations:

$$\sum_n \alpha_{nm} (\Psi_n^m, \Psi_{n'}^m) = (\Psi^m, \Psi_{n'}^m) \quad (18)$$

By restricting the number of the  $n'$  at the right-hand side and the summation at the left-hand side of Eq.(17) to  $M$  terms, the linear combination of the  $\Psi_n^m$ , obtained by solving the  $M \times M$  linear system, gives the least square approximation of  $\Psi^m$  as a linear combination of the  $\Psi_n^m$ . The solution is the best linear combination that one can obtain from the experimentally observed intensity profile using  $M$  terms in Eq. (17).

### 2.3. Validating the phase retrieval capabilities

In this subsection we discuss the retrieving capabilities of the extended Nijboer-Zernike theory. As an example we calculate the complex amplitude in the presence of low order coma  $\alpha_{31} = 0.05$  using Eq. (5); it is assumed that the first order approximation of the complex amplitude is valid. Then we show that phase retrieval is exact. The problem we have to solve is to retrieve the phase defect, i.e.  $\alpha_{31}$ , from the *3D-image intensity*.

Following the phase retrieval recipe discussed above, the first step is to form the linear system. In our example we use the first three coma terms  $n = 1, 3, 5$  to describe the aberrations of the point-spread function:

$$\begin{aligned} \alpha_{1,1}(\Psi_1^1, \Psi_1^1) + \alpha_{3,1}(\Psi_3^1, \Psi_1^1) + \alpha_{5,1}(\Psi_5^1, \Psi_1^1) &= (\Psi^1, \Psi_1^1) \\ \alpha_{1,1}(\Psi_1^1, \Psi_3^1) + \alpha_{3,1}(\Psi_3^1, \Psi_3^1) + \alpha_{5,1}(\Psi_5^1, \Psi_3^1) &= (\Psi^1, \Psi_3^1) \\ \alpha_{1,1}(\Psi_1^1, \Psi_5^1) + \alpha_{3,1}(\Psi_3^1, \Psi_5^1) + \alpha_{5,1}(\Psi_5^1, \Psi_5^1) &= (\Psi^1, \Psi_5^1) \end{aligned} \quad (19)$$

with  $\Psi^1$  the measured first harmonic and  $\Psi_1^1 \dots \Psi_5^1$  the calculated innerproduct. Next we explicitly calculate the inner products:

$$\begin{aligned} +1411 \alpha_{1,1} - 236 \alpha_{3,1} - 41 \alpha_{5,1} &= -11.8 \\ -236 \alpha_{1,1} + 320 \alpha_{3,1} - 79 \alpha_{5,1} &= +16 \\ -41 \alpha_{1,1} - 79 \alpha_{3,1} + 103 \alpha_{5,1} &= -3.9 \end{aligned} \quad (20)$$

The magnitude of the inner products depend on the sampling scheme in the  $(r, f)$ -space. The solution of Eq. (20) is:

$$\alpha_{1,1} = 0, \alpha_{3,1} = 0.05, \alpha_{5,1} = 0, \quad (21)$$

*exactly* matching the input.

In the next example we used a set of 40 random aberration coefficients  $\alpha_{nm}$  for input, as shown in the table.

Simulated phase retrieval					
Name	Term	$n$	$m$	Zernike coefficients	
Input aberrations				Retrieved	
Tilt	$Z_2$	1	1	0.0175	0.0175
Defocus	$Z_4$	2	0	-0.0187	-0.0187
Astigmatism	$Z_5$	2	2	0.0726	0.0726
Coma	$Z_7$	3	1	-0.0588	-0.0588
Spherical	$Z_9$	4	0	0.2183	0.2183
Three-point	$Z_{10}$	3	3	-0.0136	-0.0136
Astigmatism	$Z_{12}$	4	2	0.0114	0.0114
Coma	$Z_{14}$	5	1	0.1067	0.1067
Spherical	$Z_{16}$	6	0	0.0059	0.0059

⋮

Using Eq. (5) we calculated the complex amplitude and the image intensity. The phase retrieval procedure is applied and a *perfect reconstruction* results.

Why does phase retrieval using the extended Nijboer-Zernike approach works so well? The basic functions  $V_{00}^* V_{nm}$  are nearly orthogonal and the matrix to solve Zernike coefficients, similar to Eq. (20), is well conditioned. The perfect reconstruction results, provided sufficient  $(n, m)$ -terms are taken into account. Equation (5) and (13) suggests that we have neglected the quadratic intensity term in determining the Zernike coefficients. This is not the case. One can show, that the quadratic terms are orthogonal to the linear terms with respect to their dependence on  $f$  and therefore cancel on forming the linear systems for the coefficients  $\alpha_{nm}$  in Eq. (18). For this point and a further mathematical underpinning of the method is discussed elsewhere.<sup>10</sup>

### 3. EXPERIMENTAL RESULTS

#### 3.1. Microlithography Simulation Microscope results

The Microlithography Simulation Microscope (MSM 100)<sup>11</sup> emulates the optics of a scanner and is used for the evaluation of mask defects and optimisation of lithographic processes. The MSM 100 microscope is set to emulate a  $\lambda = 193$  nm,  $NA = 0.75$  scanner. The acquired through-focus aerial images of the isolated hole are transferred to an off-line computer for evaluation using home made software. We retrieved the Zernike

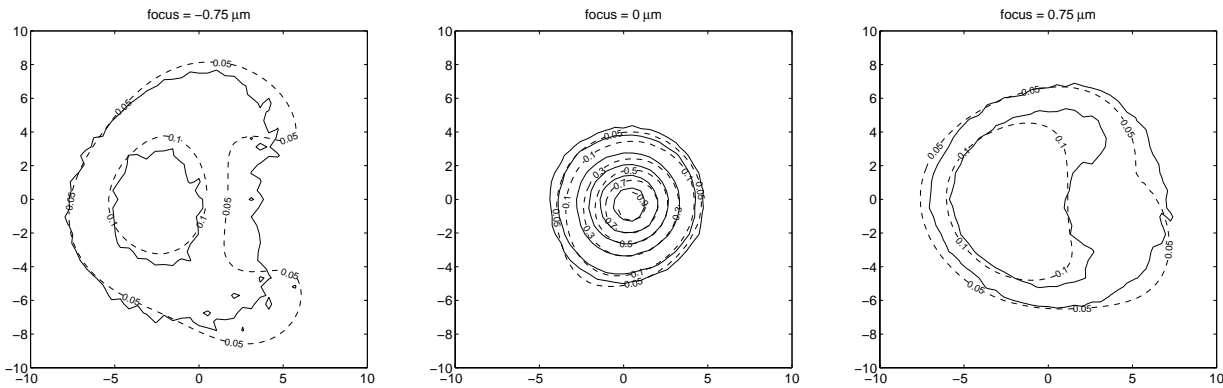


**Figure 3.** Cross sections of the MSM 100 point-spread function at various focus levels. Solid lines represent the experimental data and the dashed lines are calculated using the retrieved Zernike coefficients. High order X-coma is the dominant aberration. The  $(X, Y)$ -axis are in normalised radial units, see Eq. (1).

coefficients as described in the previous section. As a check, we calculated the image intensity using the retrieved Zernike coefficients and compared it with the experimental image intensity as shown in Fig. 3. The dominant aberration is 5<sup>th</sup>-order X-coma, which is clearly visible in the extreme defocus positions.

### 3.2. Lithographic projection lens

Getting an electronic version of the point-spread function of a scanner is somewhat more complicated. Image sensors are usually line detectors with relative broad lines having only two orientations. Even if multiple orientations would have been available, the procedure to reconstruct a point-spread function out of the image sensor signal, that essentially integrates perpendicular to the line direction, is a non-trivial procedure. Therefore we have chosen for a resist based experiment.

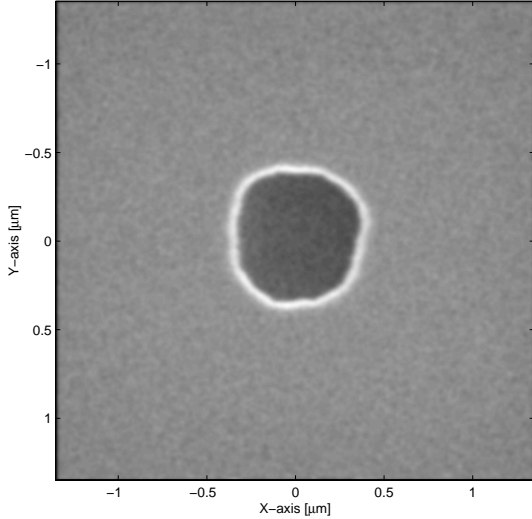


**Figure 4.** SEM image of a chrome on quartz reticle with an isolated hole, with a  $0.6 \mu\text{m}$  diameter, used in our phase retrieval experiments.

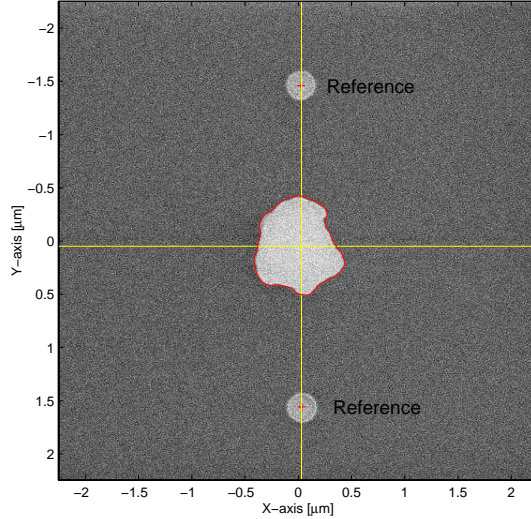


**Figure 5.** SEM image of an exposure onto resist. First two reference marks are exposed defining the coordinate system. The central image represents a single contour of the point-spread function.

The reticle, shown in Fig. 4, is a simple chrome on quartz reticle with a  $4 \times 0.15 = 0.6 \mu\text{m}$  transparent hole. An ASML PAS5500/950 system with a  $\lambda = 193 \text{ nm}$ ,  $NA = 0.63$  projection lens is used to image the reticle onto resist on a *SiON* anti-reflective coating. Using *SiON* instead of an organic anti-reflective coating has the advantage that it provides a good contrast in the SEM. First two small reference marks are exposed, using the same reticle. The coordinate system, superimposed onto the image, is shown. The relative large central image in Fig. 5 represents a single contour of the point-spread function at a certain exposure dose and defocus value. Inside this contour, the image intensity is above the resist threshold value and the resist completely develops away, leaving the *SiON* layer. Outside the contour, the SEM image shows the undeveloped resist.

The procedure is repeated for a number of focus and exposure dose settings, i.e. the reticle is exposed in a focus exposure matrix (FEM). A SEM, under job control, collects all images. The data reduction is done off-line. All contours are combined into a through-focus aerial image from which the projection lens aberrations are determined as described above. Fig. 6 shows the calculated image intensity using the retrieved Zernike coefficients compared to the experimental image intensity. The dominant terms are low order astigmatism and low order three-point.

### 3.3. Outlook: extension to general aberration retrieval

A further extension concerns the retrieval of general aberrations  $A \cdot \exp(i\Phi)$  with a possible non-constant transmission amplitude  $A$ . Now one expands

$$A \cdot \exp(i\Phi) = \sum_{n,m} \beta_{nm} R_n^m(\rho) \cos m\theta, \quad 0 \leq \theta \leq 2\pi, \quad 0 \leq \rho \leq 1. \quad (22)$$



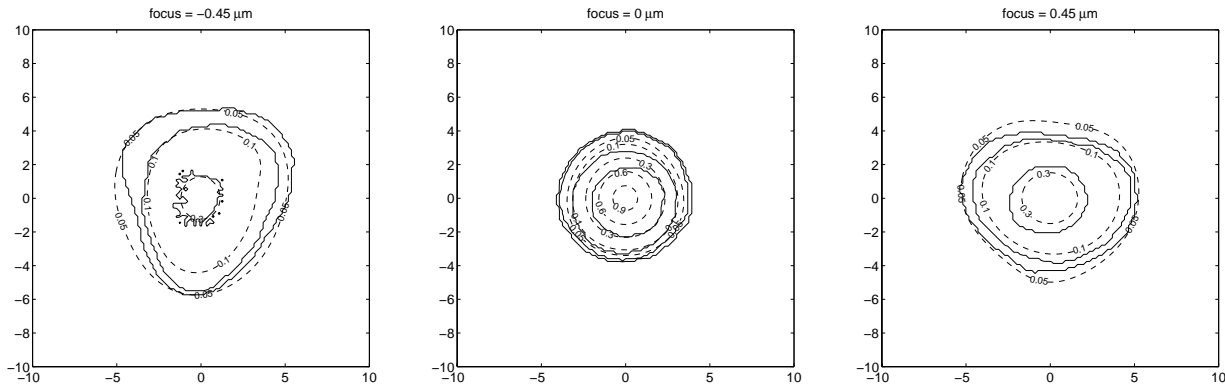


**Figure 6.** The point-spread function of a scanner reconstructed from resist images. Solid lines represent the experimental data and the dashed lines are calculated using the retrieved Zernike coefficients. Low order astigmatism and low order three-point are the dominant aberration. The  $(X, Y)$ -axis are in normalised radial units, see Eq. (1).

In case that  $A \equiv 1$  and  $\Phi$  has been expanded as in Eq. (2), one would get (under the assumption that  $\Phi$  is so small that  $\exp(i\Phi)$  may be linearized)

$$\beta_{nm} = \delta_n \delta_m + i\alpha_{nm} \quad (23)$$

with  $\delta$  Kronecker's delta. In general, we may assume that  $\beta_{00}$  is positive and large compared to the other  $\beta_{nm}$ 's. Now instead of Eq. (13) we get

$$\begin{aligned} I \approx 4\beta_{0,0}^2 |V_{00}|^2 &+ \beta_{0,0} \sum_{(n,m) \neq (0,0)} \text{Im}(\beta_{nm}) \Psi_n^m \cos m\phi \\ &+ \beta_{0,0} \sum_{(n,m) \neq (0,0)} \text{Re}(\beta_{nm}) \chi_n^m \cos m\phi \end{aligned} \quad (24)$$

Here we have, in addition to the  $\Psi_n^m$  in Eq. (16), introduced the basic functions

$$\chi_n^m(r, f) = \gamma_m \text{Re}\{i^m V_{00}^* V_{nm}\}. \quad (25)$$

Note that we now have to solve for both  $\text{Im}(\beta_{nm})$  and  $\text{Re}(\beta_{nm})$ . It turns out that the two corresponding linear systems decouple. These systems are obtained by integration over  $\phi$  as in Eq. (14) and taking inner products with  $\Psi_m^m$  and  $\chi_m^m$ , and it now happens that  $\Psi_m^m$  and  $\chi_m^m$  have opposite parity with respect to their dependence on  $f$ , their inner product vanishes. Whence in the presence of both amplitude and phase errors, two sets of linear equations must be solved instead of one. The solution is the set of  $\beta_{nm}$  coefficients that must be converted to the amplitude and phase errors using Eq. (22). Retrieval of phase and transmission is feasible and a further analysis of this extension is discussed elsewhere.<sup>10</sup>

Observe that the method as presented in section 2.2 is considerably simpler and works directly in terms of optical relevant parameters  $\alpha_{nm}$ , i.e. the Zernike coefficients. However, its applicability is restricted to the cases that we may assume negligible amplitude errors.

#### 4. DISCUSSION

In this paper we have given the proof of principle of a new experimental method to determine the aberrations of an optical system in the field. The measurement is based on the observation of the intensity point-spread function of the lens and uses an analytical method, the so-called extended Nijboer-Zernike approach for analysis and interpretation of the measurement. The new method is applicable to lithographic projection lenses, but also to microscopes such as the objective lens of an optical mask inspection tool. Phase retrieval was demonstrated both analytically and experimentally. Extension of the method to the case of a medium-to-large hole sized test object, as well as to the case of aberrations comprising both phase and amplitude errors were presented.

## ACKNOWLEDGMENTS

The authors wish to thank David van Steenwinckel, Michael Benndorf and Johannes van der Wingerden from Philips Research Leuven and Peter De Bisschop from IMEC Belgium and Alvina Williams from International Sematech USA for their valuable input and experimental support.

## REFERENCES

1. T.A. Brunner, "Impact of lens aberrations on optical lithography." *Proceedings of the Microlithography Seminar interface*, 1996 p. 1
2. D.G. Flagello, H. van der Laan, J. van Schoot, I. Bouchoms, B. Geh, "Understanding systematic and random CD variations using predictive modelling techniques.", *Proceedings of the SPIE vol. 3679*, 1999 p. 162
3. N.R. Farrar, A.L. Smith, D. Busath, D. Taitano, "In-situ measurement of lens aberrations", *Proceedings of the SPIE vol. 4000*, 2000, p. 18
4. J.P. Kirk, T.A Brunner, "Measurement of microlithography aerial image quality", *Proceedings of the SPIE vol.2726*, 1996, p. 410
5. P. Dirksen, C. Juffermans, R. Pellens, P. De Bisschop, "Novel aberration monitor for optical lithography", *Proceedings of the SPIE vol. 3679*, 1999, p. 77
6. F. Zach, C.Y. Lin, J.P Kirk, "Aberration analysis using reconstructed aerial images of isolated contacts on attenuated phase-shift masks", *Proceedings of the SPIE vol. 4346, 2001* p. 1362
7. A.J.E.M. Janssen, "Extended Nijboer-Zernike approach for the computation of optical point-spread functions", *JOSA A Vol. 19*, 2002, p. 849
8. J.J.M. Braat, P. Dirksen, A.J.E.M. Janssen, "Assessment of an extended Nijboer-Zernike approach for the computation of optical point-spread functions", *JOSA A Vol. 19*, 2002, p. 858
9. B.R.A. Nijboer, Thesis, University of Groningen (1942)
10. J.J.M. Braat, P. Dirksen, A.J.E.M. Janssen, "Retrieval of aberrations from intensity measurements in the focal region using an extended Nijboer-zernike approach", *in preparation*
11. Carl Zeiss Microelectronic systems, Germany